

Focusing of the lowest antisymmetric Lamb wave in a gradient-index phononic crystal plate

Tsung-Tsong Wu,^{1,a)} Yan-Ting Chen,¹ Jia-Hong Sun,¹ Sz-Chin Steven Lin,² and Tony Jun Huang²

¹Institute of Applied Mechanics, National Taiwan University, Taipei 106, Taiwan

²Department of Engineering Science and Mechanics, The Pennsylvania State University, University Park, Pennsylvania 16802, USA

(Received 26 January 2011; accepted 7 April 2011; published online 28 April 2011)

In this letter, we numerically demonstrate focusing of the lowest antisymmetric Lamb wave in a gradient-index phononic crystal (PC) silicon plate and its application as a beam-width compressor for compressing Lamb wave into a stubbed phononic tungsten/silicon plate waveguide. The results show that beam width of the lowest antisymmetric Lamb wave in the PC thin plate can be compressed efficiently and fitted into tungsten/silicon PC plate waveguide over a wide range of frequency. © 2011 American Institute of Physics. [doi:10.1063/1.3583660]

Over the past decade, propagation of bulk and surface acoustic waves in periodic structures called phononic crystals (PCs) has attracted a lot of interests due to the renewed physical properties of complete band gap,¹⁻⁵ negative refraction,^{6,7} etc. The existence of complete band gaps in such periodic structures has led to a variety of potential applications, such as filters,⁸ efficient acoustic waveguides,⁹⁻¹¹ and high frequency resonators.¹²⁻¹⁴ Analogous to the negative refraction of electromagnetic waves in photonic crystals,¹⁵⁻¹⁷ the counterpart of bulk acoustic waves in slab of two-dimensional PCs has also triggered intensive researches,^{6,7,18-23} and led to the research of PC-based acoustic flat lenses that can be used to focus narrow band acoustic waves for certain incident angles. By utilizing PC flat lens, reported results have demonstrated theoretically and experimentally that the resulting superlensing and imaging effects can break the diffraction limit. In addition to the bulk wave studies, investigations on the focusing of bending waves in perforated PC thin plates due to the negative refraction effect were reported.^{24,25} In spite of the complicated wave dispersion existed in thin plates, the results showed that propagation of the lowest order antisymmetric Lamb wave in PC thin plates still preserve the negative refraction features. Recently, in order to obtain focusing of bulk acoustic waves with larger bandwidth, the gradient-index (GRIN) PC has also been proposed.^{26,27} The results demonstrated that GRIN PC allows acoustic wave focusing over a wide range of operating frequencies and making it suitable for applications such as flat acoustic lenses^{28,29} and acoustic wave couplers.

In this letter, we demonstrate focusing of the lowest antisymmetric Lamb wave in a perforated GRIN PC silicon plate and its application as a beam-width compressor for compressing Lamb wave into a stubbed phononic tungsten/silicon plate waveguide.³⁰ Figure 1 shows the band structure of a thin perforated silicon³¹ PC plate with square lattice calculated by the finite element method (COMSOL MULTIPHYSICS).³² The thickness h (along z -axis) of the perforated PC plate is $50 \mu\text{m}$ while the lattice constant and the radius of the perforated holes are $a=100 \mu\text{m}$ and $r=40 \mu\text{m}$, respectively. Band structure in Fig. 1 is plotted

along the boundary of the first irreducible Brillouin zone. The solid red line shows the lowest order antisymmetric Lamb mode (A_0) and the dashed red line denotes the folded branch of A_0 mode. The symmetric Lamb mode (S_0 , solid black line) and shear horizontal mode (SH_0 , solid blue line) have much higher slopes (i.e., group velocities) than that of the A_0 mode. The inset of Fig. 1 is the equal frequency contours (EFCs) evaluated at 3 MHz. The contour of the A_0 mode is close to a circle (i.e., behaves like an isotropic medium), while the S_0 and SH_0 modes are rather anisotropic. The weakly anisotropic A_0 mode makes designing a GRIN PC plate feasible. Figure 2(a) shows band structures of the A_0 mode with different filling fraction (ff). The frequency band of the A_0 mode drops and the group velocity decreases with the increase of the ff. Figure 2(b) shows the EFCs of the A_0 mode evaluated at 3 MHz with various ffs. The EFCs show that for ff smaller than 0.503 (i.e., $r < 40 \mu\text{m}$), the contours of the A_0 mode are close to circles, meaning that anisotropy of either the phase or group velocities are small enough to be treated as weakly anisotropic.

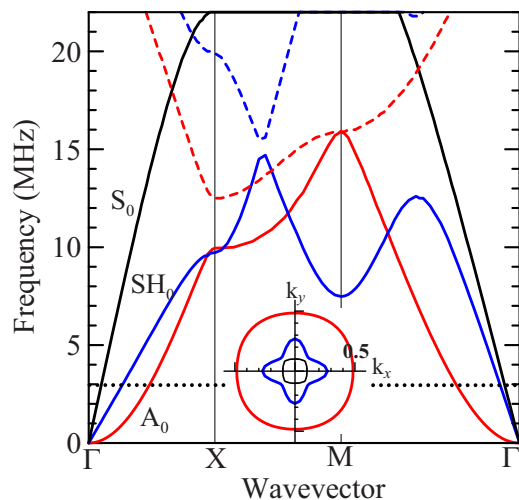


FIG. 1. (Color online) Band structure of the air/silicon PC plate with filling fraction=0.503. The inset is the EFCs at 3 MHz (dotted black line), and the wave numbers k_x and k_y are normalized by a factor of a/π .

^{a)}Electronic mail: wutt@ndt.iam.ntu.edu.tw.

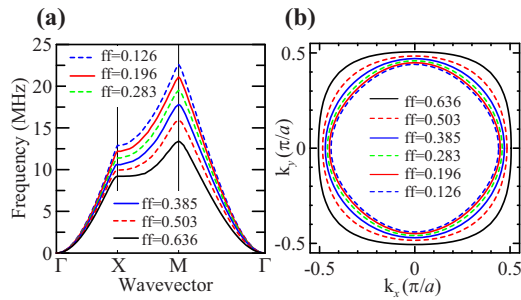


FIG. 2. (Color online) (a) Band structure of the A_0 mode of the air/silicon PC plate with different ff. (b) The EFCs of the A_0 mode shown in (a) at 3 MHz.

To design a GRIN PC plate for focusing the A_0 mode as shown in Fig. 3(a), we chose a refractive index profile in the form of a hyperbolic secant as²⁶

$$n(y) = n_0 \operatorname{sech}(\alpha y), \quad (1)$$

where n_0 is the refractive index along the x -axis and α is the gradient coefficient. For small anisotropy and the overall waves propagating along the x -direction, the refractive index of the A_0 mode is approximated by the refractive index along the ΓX direction as

$$n = \frac{v}{v_{\Gamma X}} = \frac{v}{d\omega/dk_{\Gamma X}}, \quad (2)$$

where $v_{\Gamma X}$ is the group velocity along the ΓX direction and v is the referenced group velocity of the A_0 mode of a homo-

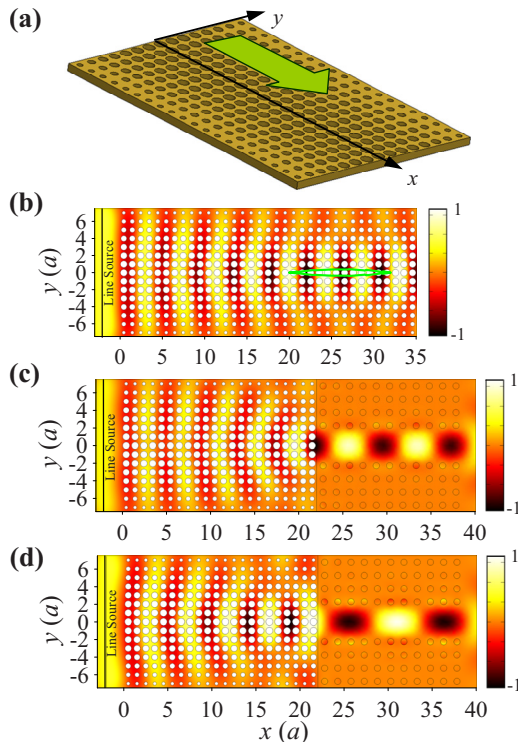


FIG. 3. (Color online) (a) A schema of the GRIN PC plate. The arrow shows the propagation direction. (b) Simulation of the wave propagation along the x -direction in the GRIN PC plate at 3 MHz. The solid contour shows the region of amplitude greater than 0.95 times of the maximum value. (c) Simulation of the wave propagation along the x -direction in a GRIN PC plate adjoining with a PC plate waveguide at 3 MHz. (d) Simulation of the wave propagation along the x -direction in the same PC structure as that in (c) at 2.7 MHz.

geneous silicon plate with the same thickness (evaluated at 3 MHz). Consider a perforated GRIN PC plate contained 15 rows of air holes ($y=[-7a, +7a]$) arranged in a square lattice with graded ffs and operated at 3 MHz. By setting the radii of the holes at the center row ($y=0$) and the boundary rows ($y=\pm 7a$) as $r=40 \mu\text{m}$ ($\text{ff}=0.503$) and $r=20 \mu\text{m}$ ($\text{ff}=0.126$), the corresponding refractive indices can be estimated as 1.159 and 1.044, respectively. The gradient coefficient was determined as $\alpha=0.665 \times 10^{-3} \mu\text{m}^{-1}$ and radii of the holes were arranged to make the effective refractive index distribution satisfies the hyperbolic secant curve.

To demonstrate focusing of the lowest antisymmetric Lamb wave (A_0) in the designed GRIN PC plate, numerical simulations were conducted with a line force placed at $x=-2a$. The result in Fig. 3(b) shows focusing of the wave beam along the propagation direction. The maximum amplitude appears at $x=28a$, which is different from the focal distance calculated by the ideal lens formula, $\pi/2\alpha$, as $x=23.6a$.²⁶ The difference of the focal lengths between the simulated and that predicted by the lens formula may come from the slightly coupling of the symmetric mode. It is worth noting that unlike the sharp focusing of the decoupled shear vertical (SV) mode of BAW in the GRIN PC, the neck of the focus region is longer. The neck region with amplitude greater than 0.95 times of the maximum amplitude is marked in Fig. 3(b) which shows the region started from $x=20a$ and ended at $x=32a$. To further study the thickness effect on the focusing behavior of the GRIN PC plate, another GRIN PC plate with $20 \mu\text{m}$ thickness was analyzed. The operating frequency was kept the same as 3 MHz, and the corresponding wavelength of the A_0 mode is $304 \mu\text{m}$ ($\lambda \approx 15h$), shorter than the one ($473 \mu\text{m}$, $\lambda \approx 10h$) in the $50 \mu\text{m}$ thickness plate. The result shows that the difference between the simulated and the predicted one is $2.3a$ which is smaller than the previous case. In addition, in the thinner GRIN PC plate, the normalized amplitude of the focal point has a higher value (2.47 for the $20 \mu\text{m}$ and 2.13 for the $50 \mu\text{m}$ case) and the neck is shorter ($x=[20a, 29a]$).

To test the feasibility of compressing the wave beam of a plate wave into a waveguide with small aperture, the GRIN PC plate with $50 \mu\text{m}$ thickness was terminated at $x=22a$ and utilized as a beam width compressor. A phononic plate waveguide is constructed on a silicon PC plate with periodic stubbed tungsten cylinders³³ (square lattice) on one of the plate surfaces by removing two layer of cylinders in the x -direction [right part of Fig. 3(c)]. The thickness of the silicon plate of the waveguide is the same as that of the GRIN PC plate ($50 \mu\text{m}$). By choosing the lattice constant of the PC waveguide as $150 \mu\text{m}$ and the radius and height of the tungsten cylinders as $36 \mu\text{m}$ and $273 \mu\text{m}$, respectively, a complete band gap can be found in the range of 2.6–3.4 MHz. Figure 3(c) shows a combination of the GRIN PC beam width compressor and the aforementioned PC waveguide. The simulation result for the operating frequency at 3 MHz demonstrates that the compressing and guiding of the wave beam into the designed waveguide can be achieved successfully. We inspected the amplitude profiles of the wave beam at different positions. By taking the amplitude of the line source as unity, the result shows that the amplitude at the entrance of the waveguide (where $x=22a$) is amplified to about 3.2. The results also show that after propagating for a distance of $15a$ in the waveguide (where $x=37a$), the wave

amplitude still preserves a value of 2.8 and the full-width at half maximum of the compressing is about 17.3%. To demonstrate that the proposed GRIN PC plate focusing device is suitable for compressing wave with a range of frequency, numerical simulations with operating frequencies at 2.7 and 3.4 MHz were also conducted and the results showed that the focusing and compressing of Lamb waves are still valid with the amplitudes at the entrance of the waveguide equal to 2.5 and 2.6, respectively. The results demonstrate that operating frequency range of the proposed GRIN PC plate wave focusing structure can be as high as 23% of the design frequency, i.e., 3 MHz. Shown in Fig. 3(d) is the simulation result for operating frequency at 2.7 MHz.

In summary, we have numerically demonstrated the focusing of Lamb wave in a GRIN air/silicon PC thin plate. The band structures of air/silicon phononic thin plate with various ffs are analyzed and discussed. We showed that the refractive index profile in the form of a hyperbolic secant can be utilized to design the GRIN PC plate and the beam width of the lowest antisymmetric Lamb mode can be compressed efficiently over a range of frequency. The results can potentially be utilized as a beam width compressor for compressing Lamb waves into a PC plate waveguide in the MEMS area.

Financial support of this research from the National Science Council of Taiwan (Grant No. NSC 99-2221-E-002-032-MY2) is gratefully acknowledged.

- ¹M. S. Kushwaha, P. Halevi, L. Dobrzynski, and B. Djafari-Rouhani, *Phys. Rev. Lett.* **71**, 2022 (1993).
- ²Y. Tanaka and S. Tamura, *Phys. Rev. B* **58**, 7958 (1998).
- ³G. Wang, X. Wen, J. Wen, L. Shao, and Y. Liu, *Phys. Rev. Lett.* **93**, 154302 (2004).
- ⁴J.-C. Hsu and T.-T. Wu, *IEEE Trans. Ultrason. Ferroelect., Freq. Contr.* **53**, 1169 (2006).
- ⁵S. Benchabane, A. Khelif, J. Y. Rauch, L. Robert, and V. Laude, *Phys. Rev. E* **73**, 065601 (2006).
- ⁶X. Zhang and Z. Liu, *Appl. Phys. Lett.* **85**, 341 (2004).
- ⁷L. Feng, X.-P. Liu, M.-H. Lu, Y.-B. Chen, Y.-F. Chen, Y.-W. Mao, J. Zi, Y.-Y. Zhu, S.-N. Zhu, and N.-B. Ming, *Phys. Rev. Lett.* **96**, 014301 (2006).

- ⁸Y. Pennec, B. Djafari-Rouhani, J. O. Vasseur, A. Khelif, and P. A. Deymier, *Phys. Rev. E* **69**, 046608 (2004).
- ⁹J.-H. Sun and T.-T. Wu, *Phys. Rev. B* **74**, 174305 (2006).
- ¹⁰F.-L. Hsiao, A. Khelif, H. Moubchir, A. Choujaa, C.-C. Chen, and V. Laude, *Phys. Rev. E* **76**, 056601 (2007).
- ¹¹J. O. Vasseur, P. A. Deymier, B. Djafari-Rouhani, Y. Pennec, and A. C. Hladky-Hennion, *Phys. Rev. B* **77**, 085415 (2008).
- ¹²T.-T. Wu, W.-S. Wang, J.-H. Sun, J.-C. Hsu, and Y.-Y. Chen, *Appl. Phys. Lett.* **94**, 101913 (2009).
- ¹³C.-Y. Huang, J.-H. Sun, and T.-T. Wu, *Appl. Phys. Lett.* **97**, 031913 (2010).
- ¹⁴S. Mohammadi, A. A. Eftekhari, W. D. Hunt, and A. Adibi, *Appl. Phys. Lett.* **94**, 051906 (2009).
- ¹⁵H. Kosaka, T. Kawashima, A. Tomita, M. Notomi, T. Tamamura, T. Sato, and S. Kawakami, *Phys. Rev. B* **58**, R10096 (1998).
- ¹⁶M. Notomi, *Phys. Rev. B* **62**, 10696 (2000).
- ¹⁷C. Luo, S. G. Johnson, J. D. Joannopoulos, and J. B. Pendry, *Phys. Rev. B* **65**, 201104 (2002).
- ¹⁸L. Feng, X. P. Liu, Y. B. Chen, Z. P. Huang, Y. W. Mao, Y. F. Chen, J. Zi, and Y. Y. Zhu, *Phys. Rev. B* **72**, 033108 (2005).
- ¹⁹M. Z. Ke, Z. Y. Liu, Z. G. Cheng, J. Li, P. Peng, and J. Shi, *Solid State Commun.* **142**, 177 (2007).
- ²⁰P. A. Deymier, B. Merheb, J. O. Vasseur, A. Sukhovich, and J. H. Page, *Rev. Mex. Fis. S* **54**, 74 (2008).
- ²¹Z. J. He, F. Y. Cai, Y. Q. Ding, and Z. Y. Liu, *Appl. Phys. Lett.* **93**, 233503 (2008).
- ²²L. Y. Wu, L. W. Chen, and R. C. C. Wang, *Physica B* **403**, 3599 (2008).
- ²³A. Sukhovich, L. Jing, and J. H. Page, *Phys. Rev. B* **77**, 014301 (2008).
- ²⁴M. Farhat, S. Guenneau, S. Enoch, A. B. Movchan, and G. G. Petursson, *Appl. Phys. Lett.* **96**, 081909 (2010).
- ²⁵J. Pierre, O. Boyko, L. Belliard, J. O. Vasseur, and B. Bonello, *Appl. Phys. Lett.* **97**, 121919 (2010).
- ²⁶S.-C. S. Lin, T. J. Huang, J.-H. Sun, and T.-T. Wu, *Phys. Rev. B* **79**, 094302 (2009).
- ²⁷S.-C. S. Lin, B. R. Tittmann, J.-H. Sun, T.-T. Wu, and T. J. Huang, *J. Phys. D: Appl. Phys.* **42**, 185502 (2009).
- ²⁸T. P. Martin, M. Nicholas, G. J. Orris, L.-W. Cai, D. Torrent, and J. Sanchez-Dehesa, *Appl. Phys. Lett.* **97**, 113503 (2010).
- ²⁹S. S. Peng, Z. J. He, H. Jia, A. Q. Zhang, C. Y. Qiu, M. Z. Ke, and Z. Y. Liu, *Appl. Phys. Lett.* **96**, 263502 (2010).
- ³⁰T.-C. Wu, T.-T. Wu, and J.-C. Hsu, *Phys. Rev. B* **79**, 104306 (2009).
- ³¹We use $C_{11}=167.5$ GPa, $C_{12}=63.9$ GPa, $C_{44}=79.6$ GPa, and density $=2332$ kg/m³.
- ³²Structural Mechanics, COMSOL MULTIPHYSICS, Manual, Comsol, AB, Stockholm, Sweden.
- ³³We use $C_{11}=503$ GPa, $C_{12}=199$ GPa, $C_{44}=152$ GPa, and density $=19200$ Kg/m³.